

# Radar-based measurement of deflections on bridges and large structures

Carmelo Gentile<sup>1</sup>

<sup>1</sup>*Department of Structural Engineering, Politecnico di Milano, Italy*  
*E-mail: gentile@stru.polimi.it*

*Keywords:* Bridge, cable, microwave interferometry.

**SUMMARY.** With the development of radar techniques, the microwave interferometry has recently emerged as an innovative technology, suitable to the non-contact vibration monitoring of large structures. New radar systems – entirely designed and developed by Italian researchers – are now available and capable of simultaneously measuring the static or dynamic deflection of several points on a large structure with sub-millimetric accuracy.

The objectives of the paper are: (a) to discuss the radar technology required to provide the measurement of deflections and (b) to illustrate the application of the new technique in ambient vibration tests of a full-scale bridge and in the measurement of the vibration response of structural elements very difficult to access by using conventional techniques, such as stay cables.

## 1 INTRODUCTION

The development of innovative non-contact systems for vibration measurement has recently drawn the attention of several researchers and especially applications of Laser Doppler vibrometer (see e.g. [1-2]), Global Positioning Systems (GPS) [3-4], and image analysis and vision-based systems using digital image processing techniques [5] are reported in the literature. Furthermore, a non-contact system using microwaves was described in [6] and used to measure the vibration response of the well-known steel composite I-40 bridge over Rio Grande river [7]; this sensor did not provide any *range resolution*, i.e. was not capable to detect different targets in the scenario illuminated by the microwave beam..

The paper is focused on a microwave interferometer recently developed [8-11] and capable of simultaneously measuring the (static or dynamic) deflection of several points of a structure with high displacement sensitivity ( $< 0.02$  mm) [9]. For the radar sensor, each discontinuity of a structure – such as the "corner zones" corresponding to the intersection of girders and cross-beams in the deck of bridges – represents a potential source of reflection of the electromagnetic waves generated by the radar and the corner zones act as a series of virtual sensors. In special cases, when the structure is not sufficiently reflective to electromagnetic waves or when displacement of specific points on the structure must be measured, simple passive radar reflectors can be quickly and easily fixed [9-10]. In addition to its non-contact feature, the microwave sensor provides other advantages including a wide frequency range of response, portability and quick set-up time.

After some preliminary tests carried out on full-scale structures [8], a joint research started between the company who developed the new radar sensor (IDS, Ingegneria Dei Sistemi, Pisa, Italy) and the Politecnico di Milano (Dept. of Structural Engineering), mainly aimed to validate the results of the equipment and to assess its performance in full-scale testing of bridges. Results of this investigation are reported in [9-11] and included:

1. establishing the actual displacement sensitivity of the equipment ( $0.01\div 0.02$  mm) through free vibration tests carried out in the laboratory on a simple spring-mass system [9];



Figure 1: View of the microwave interferometer (IDS, model *IBIS-S*).

2. verifying the stability in long term functioning (both in the laboratory and on-site), required for effective employment in static and dynamic tests or in continuous dynamic monitoring [9-11];
3. ambient vibration testing (AVT) of a reinforced concrete bridge, using simple radar reflectors placed as close as possible to conventional sensors [9-10]. The velocity time-histories evaluated from the radar sensor (and obtained by deriving the displacements) generally exhibited excellent agreement with the ones recorded by conventional sensors. Furthermore, resonant frequencies and mode shapes of the bridge, that were identified from the radar signals, turned out to be as accurate as that obtained with traditional accelerometers;
4. static testing of a steel-composite bridge [11], in order to directly compare the deflections provided by the microwave interferometer and by conventional sensors (namely LVDT extensometers).

The paper first describes the main radar techniques implemented in the sensor, in order to highlight advantages and potential issues of the new technology and to properly discuss the technical characteristics of microwave interferometers. Subsequently, the accuracy and simplicity provided by the radar techniques in the practical applications is summarized and reviewed; peculiarly, the field tests include the measurement of vibration responses on a steel-composite bridge and the vibration survey of structural elements very difficult to access by using conventional techniques, such as the cables of a cable-stayed bridge.

## 2 THE MICROWAVE INTERFEROMETER

The radar sensor used in this work is an industrially engineered micro-wave interferometer (IDS, model *IBIS-S*) and consists of a sensor module, a control PC and a power supply unit.

The sensor module (see Figure 1) is a coherent radar (i.e. a radar preserving the phase information of the received signal) generating, transmitting and receiving the electromagnetic signals to be processed in order to provide the deflection measurements. The equipment radiates at a central frequency of 16.75 GHz so that the radar is classified as  $K_u$ -band, according to the standard radar-frequency letter-band nomenclature from IEEE Standard 521-1984. The sensor unit, weighing 12 kg, is installed on a tripod equipped with a rotating head, allowing the sensor to be orientated in the desired direction, as shown in Figure 1. The module has an USB interface for connection with the control PC and an interface for the power supply module.

The control PC is provided with the software for the system management and is used to configure the acquisition parameters, store the acquired signals, process the data and view the initial results in real time. Finally, the power supply unit provides power to the system through a 12 V battery unit.

The main functions of the equipment are the simultaneous detection of the position and deflection of different targets placed at different distances from the sensor. This performance is obtained by using two well-known radar techniques:

1. the Stepped-Frequency Continuous Wave (SF-CW) technique [12], adopted to resolve the scenario in the range direction, i.e. to detect the position of different target surfaces placed along the radar's line of sight;
2. the phase Interferometry technique [13], implemented to compute the displacement of each target by comparing the phase information of the back-scattered electromagnetic waves collected at different times.

A SF-CW radar continuously transmits bursts of  $N$  electromagnetic pulses, generally named tones, whose frequencies are increased from tone to tone by a constant frequency increment  $\Delta f$ ; hence, a large effective bandwidth of  $B=(N-1)\Delta f$  is attained. A large value of  $B$  is, in turn, highly desirable since the range resolution (i.e. the minimum separation that can be detected along the radar's line of sight)  $\Delta r$  may be expressed as:

$$\Delta r = \frac{c}{2B} \quad (1)$$

where  $c$  is the speed of light in free space.

The magnitude of the IDFT of the received echoes at each time sample provides a synthetic profile (i.e. a 1-D map) of the scattering objects in the space illuminated by the antenna beam, as a function of their relative distance from the sensor. For example, Figure 2 shows an ideal range profile, or range profile, as expected when the radar beam illuminates a series of targets at different distances and different angles from the axis of the system. The peaks in the plot of Figure 2 correspond to points with good electromagnetic reflectivity; the position of these targets is clearly identified from the range (i.e. distance from the sensor) and the radar can simultaneously detect the displacement or the transient response of these points.

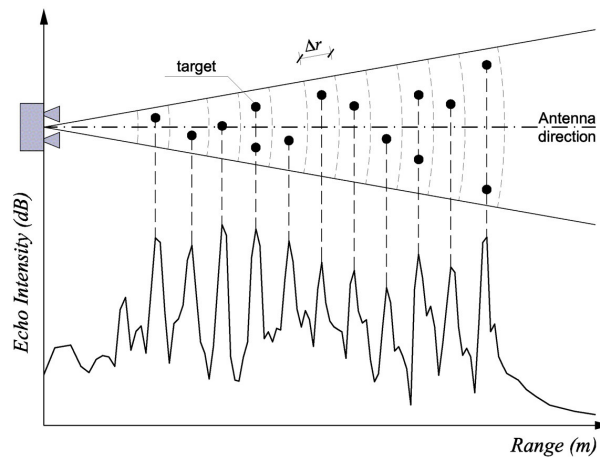


Figure 2: Idealized plot of a radar image profile (range profile).

Figure 2 also shows that the radar has only 1-D imaging capabilities, i.e. different targets can be individually detected if they are placed at different distances from the radar.

The use of step-frequency continuous waveform exhibits several advantages:

- CW radars can reach the same far distance of a pulse radar by transmitting lower power. In turn, low transmitted power generally allows SF-CW radars to be included in the Short Range Device category as a license-free use equipment;
- SF modulated radars can transmit and receive signals with precise frequency control by using Direct Digital Synthesizer, an innovative up-to-date device for generating step-frequency signals.

While the magnitude of the IDFT of the received echoes, provides the position in range of the different objects detected in the scenario, the displacement of each target object is evaluated by comparing the phase information of the electromagnetic waves reflected by the target in different time instants.

According to phase interferometry technique [13] in radar systems, when the electro-magnetic wave is reflected from a scattering object moving along the direction of wave propagation, a phase shift arises between the signals reflected by the target surface at different times. In other words, the phase of a signal received from a target depends, on its range so that the occurred range variations can be determined by evaluating the phase differences of range profiles obtained at different times. Hence, the displacement along the radar line-of-sight  $d_r$  (i.e. the radial displacement) is simply computed from the phase shift  $\Delta\vartheta$  as:

$$d_r = -\frac{\lambda}{4\pi} \Delta\vartheta \quad (2)$$

where  $\lambda$  is the wavelength of the electromagnetic signal.

Since the interferometric technique (2) provides a measurement of the radial displacement, the evaluation of the actual displacement requires the prior knowledge of the direction of motion. For many bridges (simple or continuous spans, frame or truss bridges), the displacement under traffic loads can be assumed as vertical and it can be easily evaluated by making straightforward geometric projections.

The main technical and operational characteristics of IBIS-S are summarized as follows:

1. minimum range resolution: 0.50 m;
2. maximum sampling rate: 200 Hz;
3. maximum operating distance: depending on sampling rate and range resolution [11].

Furthermore, the equipment is quick and easy to install and can be used both day and night, and in almost any weather conditions.

### 3 AMBIENT VIBRATION TEST OF A STEEL-COMPOSITE BRIDGE

#### 3.1 Description of the bridge

The investigated steel-composite bridge belongs to a motorway intersection (see Figure 3), recently completed in the neighbourhood of Forlanini Avenue, Milan, that is the main road linking the city centre to the city airport of Linate. The new infrastructure, shown in Figure 3, includes two viaducts over-passing Forlanini Avenue.

The south-side viaduct is a continuous span steel-concrete composite bridge, consisting of 8 spans; the intermediate spans are generally 50.0 m long, while the end-spans are 38.0 m long, for a total length of 376.0 m. The structure consists of ladder beams with cantilevers; hence, the cross-section is characterised by two main longitudinal girders with transverse cross-beams, at a

longitudinal spacing of 4.17 m. The cross-beams are extended beyond the girder to form cantilevers spanning 4.15 m. The girders are 2.55 m high while the floor beams are 1.00 m high. Girders and floor beams have wide flanges supporting a R/C slab 25.0 cm thick. The total width of the deck is 18.0 m for three traffic lanes and two lateral emergency lanes.



Figure 3: Aerial view of the new viaducts over Forlanini Avenue, Milan, Italy. (Courtesy of G. Massone and G. Pasqualato, Sineco S.p.A.)

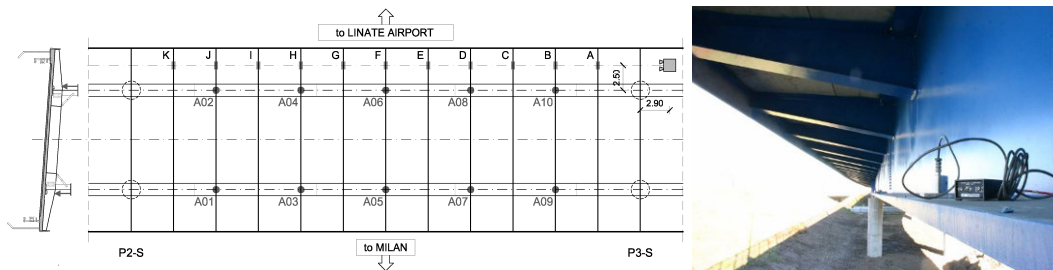


Figure 4: Forlanini Avenue over-pass: accelerometers' layout and radar position during the tests.

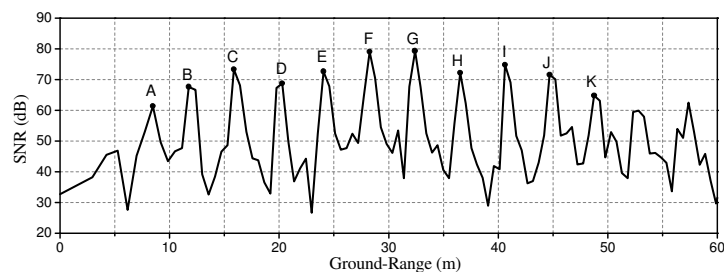


Figure 5: Forlanini Avenue over-pass: typical ground-range profile of the investigated span.

### 3.2 Experimental procedures

The ambient vibration tests were conducted using a 16-channel data acquisition system with 10 uniaxial WR-731A piezoelectric accelerometers, each with a battery power unit (see Figure 4). Since these sensors allow acceleration or velocity responses to be recorded, velocity time-histories were recorded either for operational modal analysis purposes or to enable an easier comparison with the signals acquired from the radar system.

During the tests, only the span between piers P2-S and P3-S was investigated; Figure 4 shows a schematic of the accelerometer layout on the investigated span and the position of radar sensor.

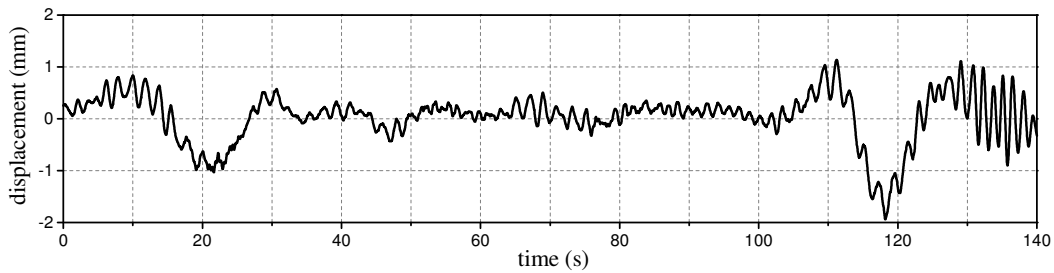


Figure 6: Forlanini Avenue over-pass: displacement time-history measured by the radar sensor.

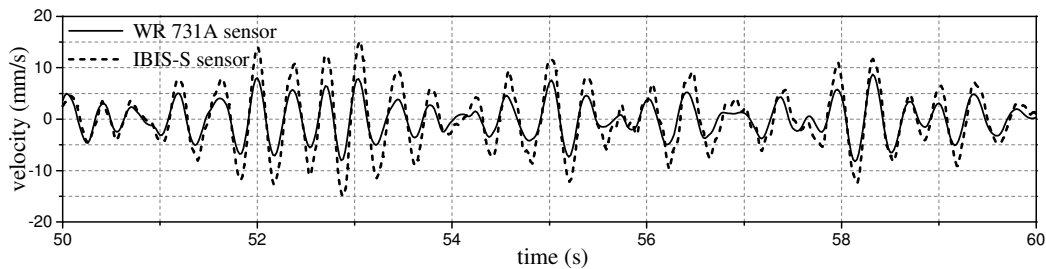


Figure 7: Forlanini Avenue over-pass: example of comparison between the velocities recorded by conventional (WR 731A) and radar (IBIS-S) sensors.

The control PC of the microwave interferometer has been configured in order to measure targets up to a distance of 80.0 m, with a scenario sampling frequency of 200 Hz and the same sampling rate was adopted for WR-731A sensors.

### 3.3 Dynamic behaviour of the bridge and results obtained from the radar sensor

The analysis of the results provided by the microwave interferometer first included the inspection of the ground range profile, shown in Figure 5. This inspection, to be performed on site, allows to verify that the sensor positioning provides a correct image of the scenario. For example, the plot in Figure 5 exhibits relative maxima of the echo intensity, clearly identifying the transverse cross-beams. It is worth underlining that the areas of the cross-beams corresponding to the peaks of Figure 5 (and hence the points where deflections are measured) are in principle placed along the radar's line of sight; this means that, since the transverse distance of the radar from pier P3-S is 2.50 m, the displacements of cross-beams are measured at a distance of 2.50 m from the pier as well (see Figure 4).

Subsequently, the deflections obtained by the radar were qualitatively examined. For example, Figure 6 shows the displacement time-history measured in correspondence of the cantilever placed at the centre of the investigated span (and marked by letter F in Figure 5).

As in previous investigations [9-11], the velocities recorded by the WR 731A sensors were compared to the velocities computed by deriving the displacement obtained from the IBIS-S sensor. An example of comparison is illustrated in Figure 7; the figure refers to the signals simultaneously recorded in the central cross-section (see sensor A06 and zone F of the cantilever of Figure 5) over a time period of 10 s. Figure 7 clearly shows that the two series of data exhibit the same in-time evolution and very similar shapes, with the radar time-history being about 30% larger than the one recorded by the conventional sensor. These amplitude differences, observed in all cross-beams over a

2260 s period, may be explained by recalling that conventional and radar measurements do not refer to the same points and are possibly related to the torsion of the deck.

The operational modal analysis of simultaneously acquired data (over a time window of 2260 s) seems to confirm the above hypothesis. 13 normal modes were identified in the frequency range 0–9 Hz by applying the FDD technique [14] to the velocity data recorded by the WR731A sensors and to the displacement data provided by the IBIS-S sensor. The identified modes are dominant bending (B) modes and dominant torsion modes (T) of the deck; due to the transverse slope of the deck, deck torsion is never negligible, even under prevailing bending.

Table 1 compares the corresponding mode shapes and scaled modal vectors through the well-known *Modal Assurance Criterion* (MAC) [15]. The natural frequencies identified from radar data turned out to be practically equal to the ones from conventional data (with the frequency discrepancy being less than 1%, as shown in Table 1). Furthermore, also the modal displacements exhibit a very good agreement, with MAC values always very close to unity (provided that the modal amplitudes are scaled to their maximum values).

Table 1. Forlanini Avenue over-pass: modal parameters identified from WR 731A and IBIS-S data.

Mode Identifier	$f$ (Hz)		MAC	Mode Identifier	$f$ (Hz)		MAC
	WR-731A	IBIS-S			WR-731A	IBIS-S	
B <sub>1</sub>	1.904	1.905	0.996	B <sub>7</sub>	3.833	3.835	0.998
B <sub>2</sub>	2.075	2.076	0.992	T <sub>2</sub>	6.055	6.058	0.994
B <sub>3</sub>	2.368	2.345	0.989	B <sub>8</sub>	6.348	6.327	0.989
B <sub>4</sub>	2.686	2.663	0.997	B <sub>9</sub>	6.641	6.645	0.985
B <sub>5</sub>	3.052	3.029	0.998	B <sub>10</sub>	6.982	6.987	0.976
B <sub>6</sub>	3.369	3.371	0.995	T <sub>3</sub>	7.251	7.280	0.984
T <sub>1</sub>	3.638	3.640	0.995	–	–	–	–

#### 4 DYNAMIC MEASUREMENT ON STAY CLABLES

The application of the radar technique to the measurement of cable vibrations seems especially promising in order to perform systematic dynamic assessment of stay cables in a simple and quick way. Peculiarly, compared to other techniques of remote sensing, the microwave interferometry exhibits various advantages:

- 1 low power transmitted;
- 2 higher accuracy;
- 3 possibility of simultaneously measuring the dynamic response of all cables in an array.

Furthermore, the possible issues that may occur in the application of the radar technique to structures practically cannot affect the radar survey of an array of cables; namely:

- a) the typical position of the sensor in the survey of an array of cables is inclined upward, as schematically shown in Figure 8(a); hence, the only targets encountered along the path of the electromagnetic waves are the stays itself so that 1-D imaging capability is perfectly adequate to the test scenario;
- b) it can assumed that the in-plane motion of the cable is orthogonal to its axis, so that the actual deflection  $d$  can be expressed as:

$$d = \frac{d_r}{\cos[\pi/2 - (\alpha_c + \alpha_s)]} \quad (3)$$

where  $\alpha_c$  and  $\alpha_s$  are the slope of the cable and of the sensor, respectively (see Figure 8(a)). In

other, words, the prior knowledge of the direction of motion is available for cable systems so that it is possible to evaluate the actual displacement from the radial one.

Finally, since it is quite easy to predict the scenario under the radar beam (see Figure 8(b)), the inspection of the range profile allows to quickly verify that the sensor positioning provides a correct image of the scenario.

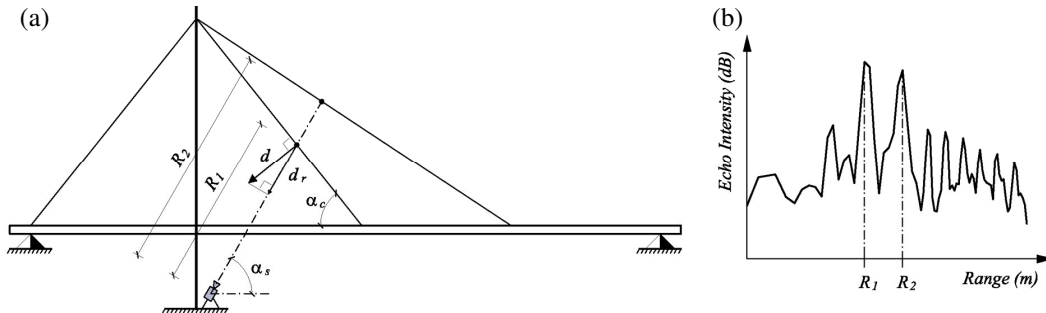


Figure 8: (a) Radial displacement versus actual (in-plane) displacement of a stay cable; (b) Typical range profile expected for an array including two cables.

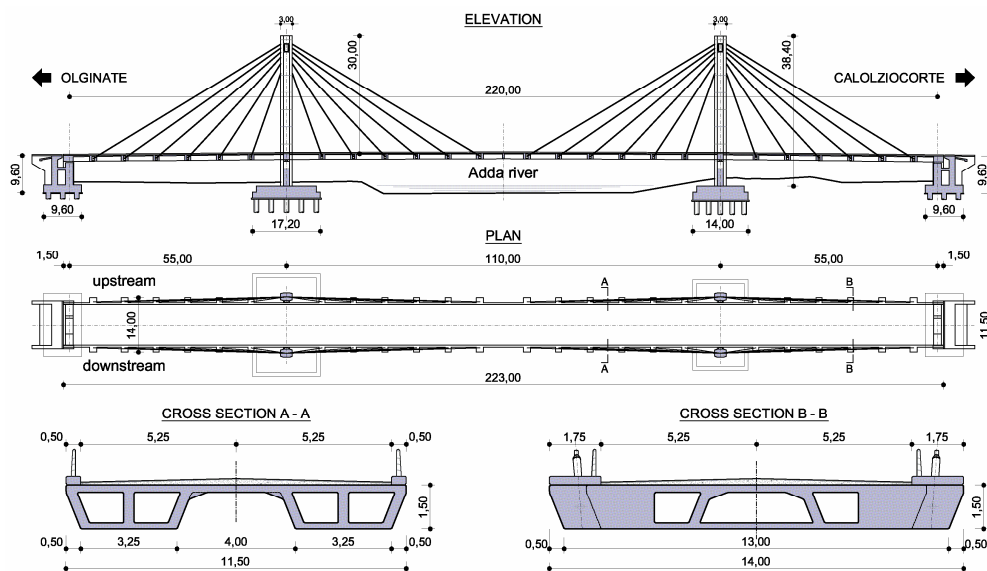


Figure 9: The "Cesare Cantù" cable-stayed bridge: elevation, plan and deck cross-sections (dimensions in m).

The accuracy and operational simplicity of the radar techniques in vibration survey of stay-cables arrays has been verified on two cable-stayed bridges: some results obtained on the longer cables of the "Cesare Cantù" cable-stayed bridge are herein after presented and discussed.

#### 4.1 Description of the bridge

The "Cesare Cantù" cable-stayed bridge (see Figure 9) is a roadway bridge that crosses the



Adda river between the municipalities of Olginate and Calolziocorte (about 60 km north-east of Milan). The bridge, with a pre-stressed concrete deck, is formed by a central span of 110.0 m and two lateral spans of 55.0 m. Elevation and plan views of the bridge and typical cross-sections are presented in Figure 9.

The cast-in-place pre-stressed concrete deck is 11.50 m wide and consists of two two-cell box girders connected by a central slab and by a series of 24 transverse cross-beams, providing the lower anchorage of the stay cables. The deck is suspended from 24 pairs of cable stays, arranged in a semi-fan and connected to two H-shaped reinforced concrete towers reaching the height of about 38.0 m above the foundations.

#### 4.2 Experimental procedures and results

After the main phase of cable tensioning, vibration measurements were carried out on all cables, by using conventional accelerometers, to check the tension forces (already monitored by load cells); also the global dynamic characteristics of the bridge were determined by AVT in order to optimize the subsequent phase of adjustment of cable forces. Afterwards, before opening the bridge to traffic, more extensive AVT of the deck and towers was carried out, as part of the bridge reception test.

Taking profit of both series of tests performed on the bridge, dynamic measurements on some cables were carried out by simultaneously using piezoelectric accelerometers and the radar system, in order to verify the reliability and accuracy of the radar technique.

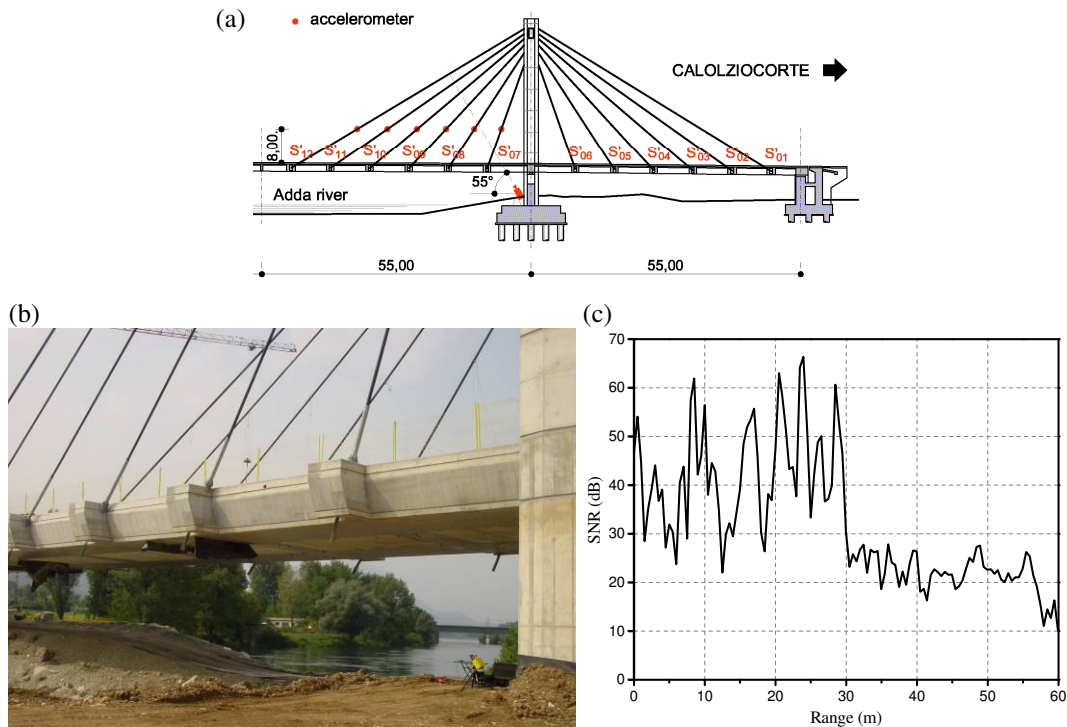


Figure 10: (a) Accelerometers' layout and radar position during the test of cables S07'-S12' (downstream side); (b) View of test scenario; (c) Range profile of the test scenario.

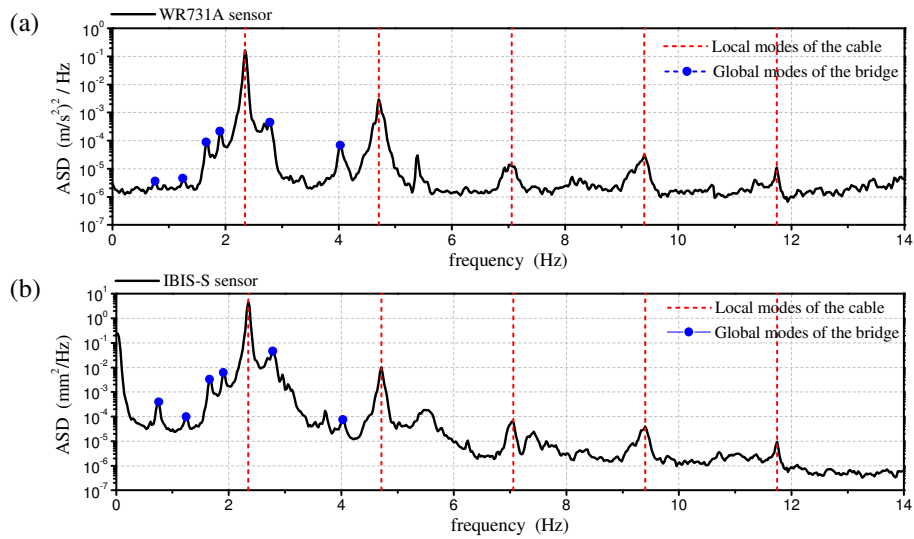


Figure 11: (a) Auto-spectrum of the acceleration data recorded on cable S12'; (b) Auto-spectrum of the displacement data measured by the radar on cable S12'.

During the tests performed after the main phase of cable tensioning, the radar system was used on two arrays of cables.

In the test of the first array, including cables S07'-S12' on the downstream side (see Figures 10(a) and 10(b)), the radar sensor was placed at base of the tower on the Calolziocorte side and inclined  $55^\circ$  upward; accelerometer and radar data were simultaneously acquired at rate of 200 Hz over a time windows of 1700 s. The range profile of the test scenario is shown in Figure 10(c); it is observed that after a first couple of peaks – placed at a range of about 10.0 m and corresponding to the concrete transverse beam providing the anchorage for cable S07' (see also the picture in Figure 10(b)) – five well defined peaks clearly identify the position of cables S08'-S12'.

Figures 11(a)-(b) show the auto-spectral densities (ASD) associated to the ambient response of cable S12', obtained from simultaneous measurements (at different points, see Figure 10(a)) of accelerometer and radar vibrometer. The ASDs were computed by using 1700 s of acquired data; smoothing was performed by 4096-points Hanning-windowed periodograms that are transformed and averaged with 66.7% overlapping, so that a total number of 124 spectral averages was obtained. Since the time interval is 0.005 s, the resulting frequency resolution is  $1/(4096 \times 0.005) \approx 0.0244$  Hz.

Although the ASDs of Figures 11(a)-(b) are associated to different mechanical quantities measured (acceleration and displacement), the spectral plots clearly highlight an excellent agreement in terms of local natural frequencies of the cable and are characterized by 5 equally spaced and well-defined peaks in the frequency range 0-12 Hz. Furthermore, some global natural frequencies of the bridge (corresponding to peaks of the ASDs placed at 0.76, 1.25, 1.68, 1.91, 2.77 and 4.02 Hz) are also apparent in Figures 11(a)-(b).

Even better results have been obtained for the second array investigated (see Figure 12), including S01-S06 cables, again on the downstream side. Although the position of the sensor and the range profile of the scenario were very similar to the previous case, a greater number of local modes have been identified, possibly due to the presence of wind excitation along the axis of the bridge during the test. For example, as shown in Figures 13(a)-(b), 12 local and equally spaced

modes have been determined for cable S02 from both conventional and radar data in the frequency range 0-35 Hz; in addition, the peaks related to the cable natural frequencies are much more evident in the ASD of radar data in the high-frequency range (7-35 Hz).

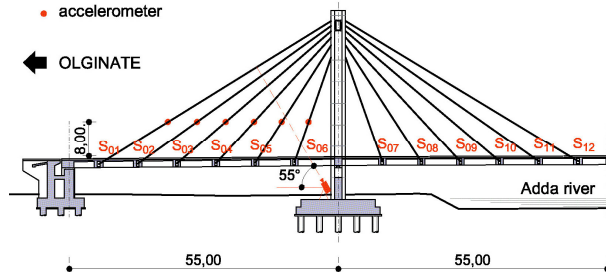


Figure 12: (a) Accelerometers' layout and radar position during the test of cables S07'-S12' (downstream side).

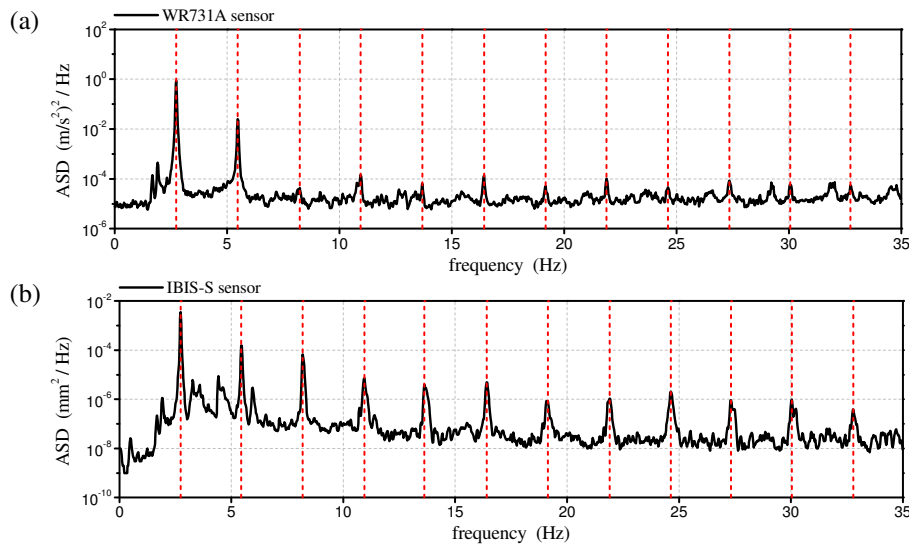


Figure 13: (a) Auto-spectrum of the acceleration data recorded on cable S02; (b) Auto-spectrum of the displacement data measured by the radar on cable S02.

## 5 CONCLUSIONS

An innovative radar sensor, developed for non contact measurements of deflections on bridges and large structures in both static and dynamic conditions, has been presented in the paper. The radar interferometer exhibited excellent stability when used on site in dynamic test of a steel-composite bridge and in ambient vibration survey of some cables of a cable-stayed bridge.

An excellent agreement was found between the modal parameters (resonant frequencies and mode shapes) identified from radar data and from data obtained with conventional accelerometers on the steel-composite bridge.

Furthermore, the radar technique turned out to be especially suitable to vibration survey of stay cables since it allows to simultaneously measure the dynamic response of several stay-cables and

provides measurements of high level of accuracy in terms of identification of natural frequencies in the cables.

#### *Acknowledgements*

The author would like to acknowledge: (1) the support provided by the Italian Ministry of University and Research (MIUR), within a National Project funded in 2006, and by IDS (Ingegneria Dei Sistemi, Pisa, Italy), owner and developer of the microwave interferometer used in the tests; (2) Dr. Giulia Bernardini (IDS) and the Local Administrations owners of the tested bridges: without their involvement and co-operation, this research would not have been possible.

#### *References*

- [1] Cunha, A. and Caetano, E., "Dynamic measurements on stay cables of cable-stayed bridges using an interferometry laser system", *Experimental Techniques*, **23**, 38-43 (1999).
- [2] Mehrabi, A.B., "In-service evaluation of cable-stayed bridges, overview of available methods, and findings", *J. Bridge Engineering*, ASCE; **11**, 716-724 (2006).
- [3] Nickitopoulou, A., Protopsalti, K. and Stiros, S., "Monitoring dynamic and quasi-static deformations of large flexible engineering structures with GPS: Accuracy, limitations and promises," *Engineering Structures*; **28**, 1471-1482 (2006).
- [4] Meng, X., Dodson, A.H. and Roberts, G.W., "Detecting bridge dynamics with GPS and triaxial accelerometers," *Engineering Structures*, **29**, 3178-3184 (2007).
- [5] Lee, J.J. and Shinozuka, M., "A vision-based system for remote sensing of bridge displacement," *NDT&E International*, **39**, 425-431 (2006).
- [6] Farrar, C.R., Darling, T.W., Migliori, A. and Baker, W. E., "Microwave interferometers for non-contact vibration measurements on large structures," *Mech. Syst. Signal Process.*, **13**, 241-253 (1999).
- [7] Farrar, C.R. and Cone, K.M., "Vibration testing of the I-40 bridge before and after the introduction of damage," in *Proc. 13<sup>th</sup> Int. Modal Analysis Conference (IMAC-XIII)*, Nashville (Tennessee), USA., February 13-16, 1995, 203-209 (1995).
- [8] Pieraccini, M., et al. 2004. "Highspeed CW step-frequency coherent radar for dynamic monitoring of civil engineering structures", *Electron. Lett.*, **40**, 907-908 (2004).
- [9] Gentile, C. and Bernardini, C., "An interferometric radar for non-contact measurement of deflections on civil engineering structures: laboratory and full-scale tests", *Structure & Infrastructure Engng.*, doi: 10.1080/15732470903068557 (2009).
- [10] Gentile, C. and Bernardini, C., "Output-only modal identification of a reinforced concrete bridge from radar-based measurements," *NDT&E International*, **41**, 544-533 (2008).
- [11] Gentile, C., "Radar-based measurement of deflections on bridges and large structures: advantages, limitations and possible applications", In *Proc. SMART'09* (invited lecture), Porto, Portugal, July 13-15, 2009, 1-20 (2009).
- [12] Wehner, D.R., *High-resolution radar*, Artech House, Norwood, MA (1995).
- [13] Henderson, F.M. and Lewis, A.J. (Eds.), *Manual of Remote Sensing. Principles and Applications of Imaging Radar*, Wiley & Sons (1998).
- [14] Brincker, R., Zhang, L.M. and Andersen, P., "Modal identification from ambient responses using Frequency Domain Decomposition", in *Proc. 18<sup>th</sup> Int. Modal Analysis Conference (IMAC-XVIII)*, San Antonio (Texas), USA., February 7-10, 2000, 625-630 (2000).
- [15] Allemang, R.J. and Brown, D.L., "Correlation coefficient for modal vector analysis", in *Proc. 1<sup>st</sup> Int. Modal Analysis Conference (IMAC-I)*, 110-116 (1983).